Analysis and Implementation of Hologram Lenses for See-Through Head-Mounted Display

Seungjae Lee, Byounghyo Lee, Jaebum Cho, Changwon Jang, Jonghyun Kim, and Byoungho Lee, *Fellow, IEEE*

Abstract—We introduce an approach to implementation of see-through head-mounted displays using hologram lenses, which are categorized by holographic optical elements. The hologram lenses magnify displayed images and superimpose the magnified images on the real-world simultaneously, which allows system configuration to be compact. Here, we investigate imaging properties and optical issues of hologram lenses using the spectral analysis of light field. Also, the astigmatism of hologram lenses is analyzed and its compensation method is proposed and verified. We conclude by describing display results and a practical application of the proposed method.

Index Terms—Holographic optical components, displays, optical device fabrication.

I. INTRODUCTION

AUGMENTED reality (AR) is a promising display technology that integrates the real-world environment and computer-generated information. Display systems for AR such as see-through head-mounted displays (HMD) are mainly composed of display modules and image combiners. Methodology to implement image combiners is the core technology, determining the display performance and economical values. Ideal image combiners would be compact, show high transmittance, and form clear virtual image of large field of view. Several approaches have been proposed for implementation of the image combiners, including applications of free form optics [1], [2], index matched optics [3], [4], diffractive [5] or holographic optical elements (HOEs) [6]–[10].

Here, we introduce an approach to realization of an image combiner using a hologram lens that is categorized by HOEs. The hologram lens can perform the roles of concave and half mirrors simultaneously, which allows system configuration to be compact. In addition, the hologram lens is thin and light weight, since it is recorded in a thin holographic film. Furthermore, the optical path of incident light is flexible so that it can be modified, which secures degree of freedom for the shape of HMD.

There have been similar works that applied HOEs for imaging lenses. See-through HMD system using a hologram lens was first reported in 1999 [6], [7]. However, this system
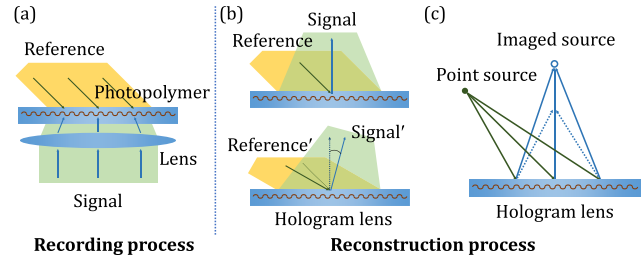
Fig. 1. (a) Recording and (b) reconstruction processes of hologram lenses: When a deviated reference wave is introduced, the signal wave is converged on a shifted focal point. (c) Illustration of image formation by hologram lenses.

suffered from optical aberrations involved by hologram lenses. Peng et al. [9] introduced a head-up compensation system that enables hologram lenses to form much clearer images. However, the size and cost of the compensation system could be a limitation in HMD. Recently, it was reported that aberration of hologram lenses can be reduced by modulation of computer generated hologram [11]. Although this method has clear merits for digital holographic displays, it is not applicable to 2-dimensional HMD. In this letter, we propose a practical approach for 2-dimensional HMD, which effectively alleviates the aberration caused by hologram lenses.

The contributions of this study are as follows: First, we establish imaging equation of hologram lenses and investigate astigmatism of hologram lenses. Second, in order to verify the analysis, the image formation by hologram lenses is simulated based on ray optics and spectral analysis of light field. Third, an optical compensation method for astigmatism of hologram lenses is proposed and verified via implementation of a prototype. We conclude with the evaluation of the prototype and a practical application of the proposed method.

II. PRINCIPLE

A. See-Through HMD Using Hologram Lenses

Hologram lenses are volume gratings that transform a specific wavefront (plane wave) to a predefined converging wavefront [12], which are fabricated via a recording process shown in Fig. 1(a). An interference pattern between reference and signal waves is recorded in a holographic material as a volume grating. The recorded hologram lens reconstructs the signal wave when the reference wave is introduced to the hologram lens. Since the signal wave is reconstructed via diffraction of the reference wave, the hologram lens can be considered as a lens that modulates the reference wave. In addition, the hologram lens can be transparent since most of wavefronts from real-world scene can pass through the hologram lens without diffraction due to the angular selectivity.

On the other hand, employing hologram lenses as imaging lenses involves optical issues. Imaging lenses can form an image of a point source by collecting light rays from the point source on another point. However, hologram lenses are designed to concentrate a specific wavefront into a focus point. When a deviated reference wave is introduced to a hologram lens, the incident wave is focused on a shifted focal point by Bragg mismatched reconstruction as shown in Fig. 1(b). Only if there is a linear relation between the incident angle of the deviated plane wave and the shifted angle of the focal point, the hologram lens could be employed as an imaging lens [11], as illustrated in Fig. 1(c). These optical issues are thoroughly analyzed in Section 3.

B. Optical Characteristics of Volume Gratings

First, we will focus on a fundamental form of volume gratings (volume Bragg grating), which can be applied to investigating optical characteristics of hologram lenses based on local approximation [13]. The fundamental grating is recorded by an interference pattern between two plane waves where the average refractive index of the volume grating is assumed as 1, for convenience in analysis. Then, the fundamental grating can be represented by a grating vector $k_g = [k_{gx}, k_{gy}, k_{gz}]$, which is given by

$$k_g = k_s - k_r, \qquad (1)$$

where k_s and k_r denote the wavevectors of signal and reference waves in the recording process, respectively. After the recording process, if a probe wave is introduced to the fundamental grating, a diffracted wave is reconstructed and its wavenumber is determined by the probe wave since the wavelength is constant.

When we consider a relatively thin volume grating represented by the superposition of infinite gratings [14], the wavevector of the diffracted wave k_d is given by

$$k_d = [k_{gx} + k_{px}, k_{gy} + k_{py}, k_{dz}], \quad |k_d|^2 = k_0^2, \qquad (2)$$

where $k_p = [k_{px}, k_{py}, k_{pz}]$ is the wavevector of the probe wave, and k_0 is the wavenumber of the probe wave. Using Eq. (2), we can derive the relationship between the probe and diffracted waves. For instance, the relationship in 2D space is given by

$$\theta_d = \sin^{-1}\left(\sin\theta_s + \sin\theta_r - \sin\theta_p\right), \qquad (3)$$

where $\theta_s, \theta_r, \theta_p$ are the incident angles of the signal, reference, and probe waves, respectively. θ_d denotes the diffracted angle of the diffracted wave.

III. HOLOGRAM LENSES

A. Imaging Equation

Using Eq. (3), we can establish the imaging equation of 1D hologram lenses in 2D space (yz plane). We consider a hologram lens that is recorded by an interference pattern between a converging wave with the focal point at $(0, f)$ and a plane wave at the incident angle of θ_r. As shown in Fig. 2, a light ray is generated from a point light source P located
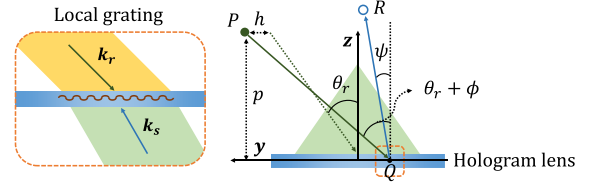

Fig. 2. Local approximation of a hologram lens to the fundamental grating.

at $(p\tan\theta_r + h, p)$ and introduced to the hologram lens at angle of $\theta_r + \phi$. As the light ray is introduced to a point $Q(q, 0)$, the light ray is transformed by the hologram lens. If we locally approximate the hologram lens as fundamental grating, Eq. (3) can be applied to determination of the transformed ray vector.

The propagation direction (ψ) of the transformed light rays is defined as follows.

$$\sin\psi = \sin(f_{\text{sig}}(q)) + \sin\theta_r - \sin(\theta_r + \phi), \qquad (4)$$

where $f_{sig}(y) = \tan^{-1}(-y/f)$ is a function that denotes local propagation directions of the converging wave recorded in the hologram lens. If ψ, ϕ, and q are sufficiently small, Eq. (4) is approximated to

$$\psi \approx f_{sig}(q) - \phi\cos\theta_r = -\frac{q}{f} - \phi\cos\theta_r. \qquad (5)$$

Therefore, optical path of the transformed rays can be described with an equation of a straight line that is given by

$$y - h + \frac{h}{f}z = \left(-p\sec^2\theta_r + \frac{zp\sec^2\theta_r}{f} - z\cos\theta_r\right)\phi, \qquad (6)$$

where q is approximated to $h - p\phi\sec^2\theta_r$. Eq. (6) is arranged relating to ϕ so that we can determine the y and z coordinates of the imaging point R that the transformed light ray passes regardless of ϕ. Accordingly, we can derive the imaging equation and magnification ratio of the hologram lens as follows.

$$\frac{1}{z} = \frac{1}{f} - \frac{\cos^3\theta_r}{p}, \quad M = -\frac{z}{p}\cos^3\theta_r, \qquad (7)$$

where z is the distance from the hologram lens to the image, and M is the magnification ratio of the hologram lens. In short, hologram lens has a distinctive imaging equation that is correlated with the term of $\cos^3\theta_r$.

B. Simulation to Investigate Imaging Property of Hologram Lenses

Analysis in the previous section is reliable when the variables ψ, ϕ, and q are sufficiently small. In order to investigate optical issues that may occur in practical applications where the variables could be large, we conduct imaging simulation in general conditions based on spectral analysis of light field [15]. Under the two-plane parameterization for 2D light field representation [16] shown in Fig. 3(a), 2D light fields or epipolar image (EPI) of a 1D object $M(y)$ that extends along the line $z = p$ is given by

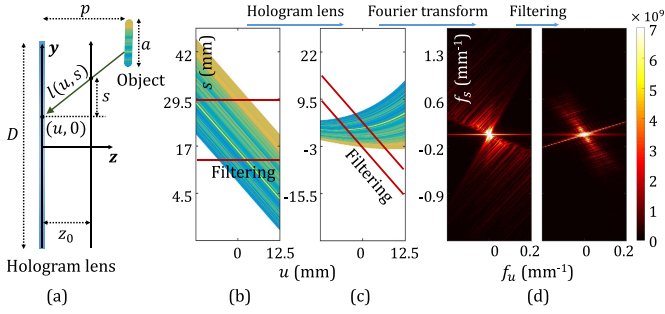$$l(u, s) = M(u + \frac{p}{z_0}s). \qquad (8)$$

Fig. 3. (a) Two-plane parameterization for 2D light field representation. EPI of (b) an object and (c) its image formed by a hologram lens, where $D = 25$ mm, $a = 25$ mm, $p = 29.46$ mm, $f = 100$ mm, and $z_0 = 20$ mm. (d) Fourier transformed EPI of the image.
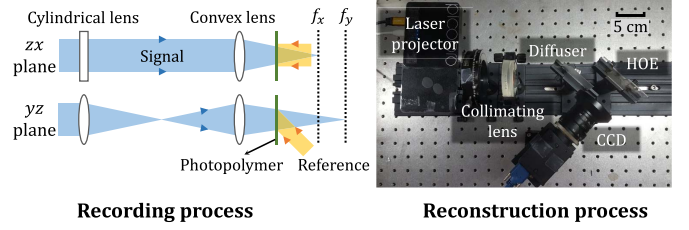

Fig. 4. Implementation of a prototype: recording and reconstruction processes. Two different lens curvatures are recorded according to the sagittal (zx) and transverse planes (yz) to alleviate astigmatism of hologram lens: Lens 1 has $f_x = f_y = 100$ mm, Lens 2 has $f_x = 45$ mm, $f_y = 100$ mm, and Lens 3 has $f_x = 50$ mm, $f_y = 105$ mm.

Fourier transform of light field $l(u, s)$ from the constant depth of p is given by

$$L(f_u, f_s) = 2\pi L_0 \delta(-\frac{p}{z_0} f_u + f_s), \qquad (9)$$

where L_0 is the 1D Fourier transform of light field $l(u, 0)$, and $\delta(\cdot)$ is the Dirac delta function. Details of this derivation can be consulted in the spectral analysis paper [17]. Eq. (9) shows that EPI of the 1D object with the constant depth is represented by a straight line in the frequency domain. Also, the slope of the straight line is determined by the depth of the object. If a 1D object has a varying depth between the z_{min} and z_{max} due to optical aberration, the EPI of the object is bounded in the frequency domain by two straight lines given by

$$g_{min} : -\frac{z_{min}}{f} f_u + f_s = 0, \quad g_{max} : -\frac{z_{max}}{f} f_u + f_s = 0. \qquad (10)$$

Figs. 3(b)-3(d) describe the imaging simulation of 2D light fields from a 1D object. First, 2D light fields of a plane object, which occupies a line segment, are constructed. The light field information is transformed by a hologram lens with the diameter of D and the focal length of f. Note that the transformed light field information denotes the EPI of an image of the plane object. Fig. 3(d) shows that the EPI of the image fills a triangular region in the frequency domain, which indicates the optical aberration of the hologram lens. However, if we employ a low-pass filter that limits diffusing angle of the plane object, the optical aberration of the hologram lens can be alleviated. When the diffusing angle is limited to 2.5°, the transformed light field shows a local part of the original field, and its Fourier transform approximately forms the shape of a straight line.

C. Astigmatism

The imaging equation of the 1D hologram lenses can be applied to investigating imaging properties of 2D hologram lenses in 3D space. In this letter, we cover a specific example of 2D hologram lens for the simplicity of analysis, which can be extended to general hologram lenses. We suppose a 2D hologram lens on xy plane, which is recorded by employing a converging wave with the focal point at $(0, 0, f)$ and a plane wave with the wavevector of $k_0[0, -\sin\theta_r, -\cos\theta_r]$.

According to Eq. (1), the local grating vector of the hologram lens is given by

$$k_g(a, b, 0) = k_s(a, b, 0) - k_0[0, -\sin\theta_r, -\cos\theta_r],$$
$$k_s(a, b, 0) = \frac{k_0}{(a^2 + b^2 + f^2)^{1/2}}[-a, -b, f], \qquad (11)$$

where $k_g(a, b, 0)$ and $k_s(a, b, 0)$ denote the local grating vector and wavevector of the signal wave at the point $(a, b, 0)$ on the hologram lens. When a probe wave with a wavevector of $k_0[-\cos(\theta_r + \phi_y)\sin\phi_x, -\sin(\theta_r + \phi_y), -\cos(\theta_r + \phi_y)\cos\phi_x]$ is introduced to the hologram lens, a diffracted wave is reconstructed, which can be derived by substituting Eq. (11) in Eq. (2).

We analyze imaging properties of the 2D hologram lens by dividing it into two perpendicular x and y sub-hologram lenses. The y sub-hologram lens is defined in the yz plane, referred to as the transverse plane where a and ϕ_x are constant. On the other hand, the x sub-hologram lens is defined in the zx plane, referred to as the sagittal plane where b and $\theta_r + \phi_y$ are constant. Applying paraxial approximation to each case, we can derive two different imaging equations according to the sagittal and transverse planes.

$$\frac{1}{z_x} = \frac{1}{f} - \frac{\cos\theta_r}{p}, \quad \frac{1}{z_y} = \frac{1}{f} - \frac{\cos^3\theta_r}{p}, \qquad (12)$$

where a point source is placed at $P(0, p\tan\theta, p)$. Consequently, two images of the point source at P are formed by the y and x sub-hologram lenses, referred to as the astigmatism of the hologram lens. This astigmatism can be optically compensated in the recording process. For instance, we can employ a converging wave that focuses on two different points in the sagittal and transverse planes. When θ_r is 45°, the converging wave should satisfy following condition to compensate astigmatism.

$$\frac{1}{f_x} - \frac{2}{f_y} = -\frac{1}{z}, \quad (z_x = z_y = z) \qquad (13)$$

where f_x and f_y denote focal points of the converging wave in the sagittal and transverse planes, respectively.

IV. EXPERIMENTS

A. Prototype Implementation of See-Through HMD

A prototype of see-through HMD is implemented as shown in Fig. 4. In the recording process, a converging wavefront
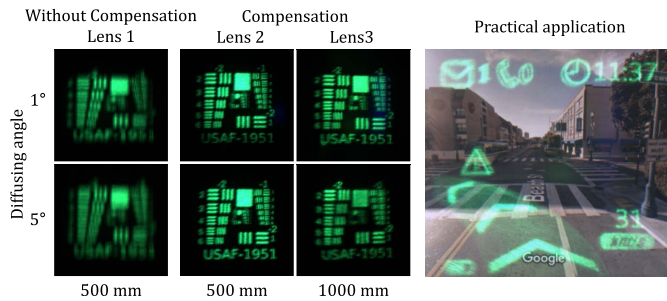
Fig. 5. Left: Astigmatism compensation and imaging performance of hologram lenses. Right: Practical application of the prototype.

from spherical and cylindrical lenses is recorded in a photopolymer. The cylindrical lens is employed for recording different lens curvatures in the sagittal and transverse planes. We use a green laser (532 nm) for coherent light source. A reference wave of the plane wavefront is introduced to the photopolymer at the incident angle of 45°. Three different lenses are implemented and analyzed: lens 1 has the same curvatures in the two perpendicular planes; lenses 2 and 3 have different curvatures that are designed for the imaging distance of 500 and 1000 mm, respectively.

The reconstruction system is composed of projection module, diffuser, and hologram lens. The projection module is divided into a laser projector and a collimating lens. The laser projector has a green light source with single wavelength of 522 nm. The collimating lens converts a diverging beam from the laser projector to a collimated projection beam. Since the projection beam is scattered by the diffuser, we can consider that a plane object is floated on the diffuser. We utilize holographic diffusers from Edmund with a limited diffusing angle that functions as the low-pass filter. The hologram lens forms an image of the plane object that can be dynamically changed by laser projector. The prototype is designed for single eye, which can be duplicated for stereoscopic HMD.

B. Evaluation

We evaluate the astigmatism compensation method and investigate imaging performance of the prototype as described in Fig. 5. For comparison, images formed by an ordinary hologram lens (lens 1) are presented. According to the images, the lens 1 shows blurred image since only horizontal information is focused at 500 mm while vertical information is focused at 70 mm. On the other hand, lenses 2 and 3 are implemented via the compensation method. Each lens has different focal points at the sagittal and transverse planes as described in Fig. 5. Compared to the lens 1, lenses 2 and 3 form clearer images with the reduced astigmatism.

Transparency and an application of the prototype are also described in Fig. 5. We mimic a navigation system using the prototype. A printed Google street view is used for background and placed at 500 mm from a camera. As shown in the results, the real-world scene of high contrast and brightness is observed beyond the hologram lens (lens 2 in Fig. 5).

Detailed specifications of the prototype are described as follows: The diffuser has the diffusing angle of 5°, which guarantees pupil size of 13 mm. The virtual image floated by the prototype has field of view (FOV) of 18° × 18°. The thickness of the hologram lens is less than 2 mm. Ghost effect is observed in the prototype, which can be alleviated using anti-reflection glasses.

V. Conclusion

We proposed a novel approach to implementation of see-through HMD using hologram lenses for realization of AR. We have improved imaging properties of hologram lenses in a practical and economical way by recording a modified converging wave and employing low-pass filtering. A prototype was implemented in order to show the validity of the proposed system and verify the compensation method. We expect that our method could be an effective way to implement see-through HMD and give novel inspirations for the realization of advanced methods.

References

[1] Q. Wang, D. Cheng, Y. Wang, H. Hua, and G. Jin, "Design, tolerance, and fabrication of an optical see-through head-mounted display with free-form surface elements," *Appl. Opt.*, vol. 52, no. 7, pp. C88–C99, Mar. 2013.

[2] X. Hu and H. Hua, "High-resolution optical see-through multi-focal-plane head-mounted display using freeform optics," *Opt. Exp.*, vol. 22, no. 11, pp. 13896–13903, 2014.

[3] J.-Y. Hong *et al.*, "See-through multi-projection three-dimensional display using transparent anisotropic diffuser," *Opt. Exp.*, vol. 24, no. 13, pp. 14138–14151, Jun. 2016.

[4] J. Hong *et al.*, "3D/2D convertible projection-type integral imaging using concave half mirror array," *Opt. Exp.*, vol. 18, no. 20, pp. 20628–20637, Sep. 2010.

[5] T. Levola, "Novel diffractive optical components for near to eye displays," in *SID Int. Symp. Dig. Tech. Papers*, Jun. 2006, vol. 37. no. 1, pp. 64–67.

[6] T. Ando, T. Matsumoto, H. Takahasihi, and E. Shimizu, "Head mounted display for mixed reality using holographic optical elements," *Memoirs-Faculty Eng.*, vol. 40, pp. 1–6, Sep. 1999.

[7] I. Kasai, Y. Tanijiri, E. Takeshi, and U. Hiroaki, "A practical see-through head mounted display using a holographic optical element," *Opt. Rev.*, vol. 8, no. 4, pp. 241–244, 2001.

[8] E. Tolstik *et al.*, "Pmma-pq photopolymers for head-up-displays," *IEEE Photon. Technol. Lett.*, vol. 21, no. 12, pp. 784–786, Jun. 2, 2009.

[9] H. Peng *et al.*, "Design and fabrication of a holographic head-up display with asymmetric field of view," *Appl. Opt.*, vol. 53, no. 29, pp. H177–H185, Sep. 2014.

[10] J. Han, J. Liu, X. Yao, and Y. Wang, "Portable waveguide display system with a large field of view by integrating freeform elements and volume holograms, " *Opt. Exp.*, vol. 23, no. 3, pp. 3534–3549, Feb. 2015.

[11] G. Li, D. Lee, Y. Jeong, J. Cho, and B. Lee, "Holographic display for see-through augmented reality using mirror-lens holographic optical element," *Opt. Lett.*, vol. 41, no. 11, pp. 2486–2489, May 2016.

[12] D. H. Close, "Holographic optical elements," *Opt. Eng.*, vol. 14, no. 5, p. 145402, Oct. 1975.

[13] S. A. Benton and V. M. Bove, Jr., *Holographic Imaging*. New York, NY, USA: Wiley, 2008.

[14] J. W. Goodman, *Introduction to Fourier Optics*. Englewood, CO, USA: Roberts and Company Publishers, 2005.

[15] J.-X. Chai, X. Tong, S.-C. Chan, and H.-Y. Shum, "Plenoptic sampling," in *Proc. ACM SIGGRAPH*, 2000, pp. 307–318.

[16] S. J. Gortler, R. Grzeszczuk, R. Szeliski, and M. F. Cohen, "The lumigraph," in *Proc. ACM SIGGRAPH*, 1996, pp. 43–54.

[17] S.-C. Chan and H.-Y. Shum, "A spectral analysis for light field rendering," in *Proc. Int. Conf. Image Process. (ICIP)*, vol. 2. 2000, pp. 25–28.